JB
Journals.ASM.org

Transcriptional Regulation of the *ecp* Operon by EcpR, IHF, and H-NS in Attaching and Effacing *Escherichia coli*

Verónica I. Martínez-Santos,[a] Abraham Medrano-López,[a] Zeus Saldaña,[b] Jorge A. Girón,[b] and José L. Puente[a]

Departamento de Microbiología Molecular, Instituto de Biotecnología, Universidad Nacional Autónoma de México, Cuernavaca, México,[a] and Department of Molecular Genetics and Microbiology, Emerging Pathogens Institute, University of Florida, Gainesville, Florida, USA[b]

Enteropathogenic (EPEC) and enterohemorrhagic (EHEC) *Escherichia coli* are clinically important diarrheagenic pathogens that adhere to the intestinal epithelial surface. The *E. coli* common pili (ECP), or meningitis-associated and temperature-regulated (MAT) fimbriae, are ubiquitous among both commensal and pathogenic *E. coli* strains and play a role as colonization factors by promoting the interaction between bacteria and host epithelial cells and favoring interbacterial interactions in biofilm communities. The first gene of the *ecp* operon encodes EcpR (also known as MatA), a proposed regulatory protein containing a LuxR-like C-terminal helix-turn-helix (HTH) DNA-binding motif. In this work, we analyzed the transcriptional regulation of the *ecp* genes and the role of EcpR as a transcriptional regulator. EHEC and EPEC *ecpR* mutants produce less ECP, while plasmids expressing EcpR increase considerably the expression of EcpA and production of ECP. The *ecp* genes are transcribed as an operon from a promoter located 121 bp upstream of the start codon of *ecpR*. EcpR positively regulates this promoter by binding to two TTCCT boxes distantly located upstream of the *ecp* promoter, thus enhancing expression of downstream *ecp* genes, leading to ECP production. EcpR mutants in the putative HTH DNA-binding domain are no longer able to activate *ecp* expression or bind to the TTCCT boxes. EcpR-mediated activation is aided by integration host factor (IHF), which is essential for counteracting the repression exerted by histone-like nucleoid-structuring protein (H-NS) on the *ecp* promoter. This work demonstrates evidence about the interplay between a novel member of a diverse family of regulatory proteins and global regulators in the regulation of a fimbrial operon.

Enteropathogenic (EPEC) and enterohemorrhagic (EHEC) *Escherichia coli* are intestinal pathogens that colonize the small gut and colon, respectively. EPEC is a major cause of infantile diarrhea, affecting principally children under 6 months of age in developing countries (51), while EHEC is a causative agent of hemorrhagic colitis (60) and the often-lethal hemolytic-uremic syndrome (HUS) (34). Both pathogens adhere to the host epithelial cells and inject effector proteins through a specialized secretion system called the type three secretion system (T3SS), leading to the formation of a distinctive histopathology known as the "attaching and effacing" (A/E) lesion. A/E lesion formation is characterized by the intimate adherence of the bacteria to the intestinal epithelium, which is mediated by the interaction between Tir and intimin; the effacement of the enterocyte microvilli; and the formation of a typical pedestal-like structure composed mainly of polymerized actin (11). Prior to these events, EPEC uses a type IV pilus, called a bundle-forming pilus (BFP) (27), to adhere to epithelial cells in a pattern known as localized adherence (LA) (32). In the case of EHEC, several fimbrial and nonfimbrial adhesins that contribute to adherence have been described, among which are the *E. coli* common pilus (ECP) (57), also called meningitis-associated and temperature-regulated (Mat) fimbriae in newborn meningitis-associated *E. coli* (NMEC) (53); the *E. coli* YcbQ laminin-binding fimbriae (ELF) (64); two long polar fimbriae (LPF) (19, 70); the F9 fimbriae (43); a type 4 pilus called "hemorrhagic coli pilus" (HCP) (77); curli (35, 62); the outer membrane proteins intimin (18) and OmpA (71); the EHEC factor for adherence (Efa1) (52); and the IgrA homologue adhesin (Iha) (69).

Fimbriae facilitate bacterial attachment to host tissues (23), which is one of the initial steps in colonization (54, 66). These structures are involved in bacterial aggregation (54) and biofilm formation (reviewed in reference 74) and contribute to bacterial virulence (54). We have recently shown that the ECP is conserved in, and expressed by, the majority of pathogenic and nonpathogenic *E. coli* strains when cultured in tissue culture medium [e.g., Dulbecco's modified Eagle's medium (DMEM)] either at 26°C or 37°C and contributes to EHEC adherence to host epithelial cells (57) and to colonization of baby spinach leaves (63). In EPEC, along with BFP and other adhesins, ECP is involved in the interaction of the bacteria with host epithelial cells (61). ECP has also been shown to play a critical role in biofilm formation by NMEC isolate IHE 3034 (38) and in colonization of the infant mouse intestine by the *E. coli* commensal strain Nissle 1917 (37). The optimal environmental and nutritional conditions for ECP production may vary among the different pathogroups. For example, NMEC produces ECP when grown at 20°C in Luria-Bertani (LB) broth (53), whereas in enterotoxigenic *E. coli* (ETEC) the pili are better produced after growth in pleuropneumonia-like organism (PPLO) broth at 37°C (6).

ECP (Mat) assembly into filamentous structures requires the function of all 6 genes composing the *ecp* operon (26, 38), which share the standard organization of fimbrial operons of the chaperone/usher pathway (30). The pili are built of a major structural subunit called EcpA (MatB), which is encoded by the second gene of the *ecp* (*mat*) operon, *ecpA* (*matB*) (26). The first gene, *ecpR*

Received 25 May 2012 **Accepted** 9 July 2012
Published ahead of print 13 July 2012
Address correspondence to José L. Puente, puente@ibt.unam.mx.
Supplemental material for this article may be found at http://jb.asm.org/.

doi:10.1128/JB.00915-12

(*matA*), codes for the EcpR (MatA) protein, which is proposed to be a regulatory protein since it contains a putative LuxR-like C-terminal helix-turn-helix (HTH) DNA-binding motif (53, 57). Proteins of this family are composed of two functional domains (50) and bind to DNA in a dimeric state, and some act as either classical transcriptional activators or transcriptional repressors in the presence or absence, respectively, of their cognate signal (50).

Proteins from this family are not commonly involved in transcriptional regulation of fimbrial operons or virulence genes in *E. coli*. However, in addition to specific regulators often encoded within each operon (4, 36), the expression of fimbrial operons is also affected by global regulators, such as the integration host factor (IHF) (22), the histone-like nucleoid-structuring protein (H-NS) (76) and the leucine-response regulatory protein (Lrp) (7, 24, 73).

In this study, we determined the function of EcpR as a positive regulator of its own expression and thus of the entire *ecp* operon in attaching and effacing *E. coli*. Deletion and site-directed mutational analysis, as well as *in vivo* footprinting, of the *ecp* regulatory region allowed the identification of regions involved in positive and negative regulation, as well as a sequence element consisting of two 5-bp direct repeats (TTCCT) distantly located at positions −189 to −185 and −211 to −207, with respect to the transcriptional start site, which are individually essential for EcpR-mediated activation. We also showed that IHF is essential for *ecp* expression and for counteracting the repression exerted by H-NS.

MATERIALS AND METHODS

Bacterial strains, plasmids and growth conditions. The bacterial strains and plasmids used in this work are described in Table 1. Overnight cultures were grown at 37°C in Luria-Bertani (LB) broth with shaking. Dulbecco's modified Eagle's medium (DMEM) containing 0.45% (wt/vol) glucose and L-glutamine (584 mg/liter), but without sodium pyruvate (Gibco BRL Life Technologies) and supplemented with pyridoxal (4 mg/ml), was used for growth at 37°C with shaking or 30°C in static conditions. When necessary, antibiotics were added at the following concentrations: ampicillin (Amp), 100 mg/ml; kanamycin (Km), 30 mg/ml; tetracycline (Tc), 15 mg/ml; chloramphenicol (Cm), 30 mg/ml; and streptomycin (Stp), 100 mg/ml.

Molecular biology techniques. DNA manipulations were performed according to standard protocols. Restriction and DNA-modifying enzymes were obtained from Invitrogen and used according to the manufacturers' instructions. Radiolabeled nucleotides ([γ-^{32}P]dATP at 3,000 Ci mmol^{-1}) were purchased from Amersham Corp. The oligonucleotides used for amplification by the PCR and for primer extension were synthesized by the Oligonucleotide Synthesis Facility at Instituto de Biotecnologia (UNAM, Cuernavaca, Mexico). PCRs were performed in volumes of 100 or 50 μl with *Taq* polymerase (Perkin-Elmer) according to the manufacturers' instructions. Sequencing reactions of the plasmids generated in this work were carried out by the dideoxy chain termination procedure (65) using a Thermo Sequenase cycle sequencing kit according to the manufacturers' instructions (Amersham, Inc.) or performed at the Core Sequencing Facility at Instituto de Biotecnologia (UNAM, Cuernavaca, Mexico).

RNA isolation and primer extension analysis. Total RNA was isolated from samples of cultures of EPEC E2348/69 and EHEC EDL933 containing fusions ecpRA-P and ecpRA-H, respectively, grown up to an optical density at 600 nm (OD_{600}) of 1.0 using an RNeasy kit (Qiagen) according to the manufacturers' instructions. The RNA concentration and quality were determined by measuring the A_{260} and A_{280}. Primer extension reactions were performed as described previously (44), with some modifications. Briefly, synthetic primer ecpR-Rev, complementary to the 5′ *ecpR* coding region, was end labeled using T4 DNA kinase (Invitrogen) and [γ-^{32}P]ATP. Labeled primer was hybridized with 10 μg of total bacterial RNA and reverse transcribed for 90 min at 37°C using MLV reverse transcriptase (Invitrogen). The resulting cDNA was resolved through a sequencing gel and bands were visualized on Kodak X-Omat film.

Reverse transcription-PCR. Transcription of *ecpA* was assessed by reverse transcription-PCR (RT-PCR) using total RNA obtained from bacteria growing in DMEM for 6 h and the oligonucleotides listed in Table S1 in the supplemental material. Bacterial RNA was extracted as recommended by the manufacturer (Macherey-Nagel). First-strand cDNA synthesis was accomplished using One Step enzyme mix containing reverse transcriptase by following the manufacturer's protocol (Qiagen). Fifty nanograms of total RNA was used for each RT-PCR. Reverse transcription was carried out at 50°C for 30 min. Reaction mixtures containing no reverse transcriptase were used as negative controls.

Construction of mutant strains. Construction of mutant strains of EPEC E2348/69 and EHEC EDL933 was performed using the one-step gene inactivation method (17) using primers listed in Table S1 in the supplemental material. Strains containing plasmid pKD46 were electroporated with the PCR products, and the mutants were selected in LB plates containing Km. Replacement of the *ecpR* gene by the Km resistance cassette was verified by PCR using adjacent primers (see Table S1 in the supplemental material). To generate strain EHEC EDL933 Δ*ecpR*, the Km cassette was removed from the EDL933 Δ*ecpR*::Km strain using plasmid pCP20 (17).

Construction of *ecpR-cat* and *ecpA-cat* transcriptional fusions and plasmids expressing EcpR. Different oligonucleotides complementary to the regulatory and coding regions of *ecpR* and *ecpA* were designed to amplify by PCR various fragments that span different portions of the regulatory region (see Table S1 in the supplemental material). PCRs were performed using chromosomal DNA from wild-type EPEC E2348/69 or EHEC EDL933 as the template. The PCR fragments were digested with BamHI and HindIII (Invitrogen) and ligated into plasmid pKK232-8, which contains a promoterless *cat* gene (Pharmacia LKB Biotechnology), digested with the same enzymes. The positions of the sequence encompassed by each fusion with respect to the transcriptional start site of the *ecp* operon are indicated in Table 1. Fusions ecpR-4m1, ecpR-4m3, ecpR4-m4, ecpR-4IRm1, and ecpR-4IRm2 were constructed by overlapped PCR using primers upEBS-F and upEBS-R, EBS-F and EBS-R, ecpRm4-F and ecpRm4-R, IHFBS-F and IHFBS-R, and IHFm-F and IHFM-R, respectively (Table S1), and plasmid pecpR-4 as the template. First, the individual products were amplified with pKK-8-BHI and the respective reverse primers and with the respective forward primers and pKK-8-H3R. The products were cleaned with DNA Clean & Concentrator Kit (Zymo Research) according to the manufacturers' instructions. The cleaned products were used for the overlapped PCR with primers pKK-8-BHI and pKK-8-H3R. Fusion ecpR-4m2 was generated by overlapped PCR using primers EBSm2-R and pKKAp59F (see Table S1 in the supplemental material) to generate the first fragment and primers EBSm2-F and pKK-8-H3R (Table S1) to amplify the second, using plasmid pecpR-4 as the template. Both fragments were used as the template for a second PCR with primers pKK-8-BHI-F and pKK-8-H3R. In all cases the resulting fragments were digested with enzymes BamHI and HindIII and cloned into plasmid pKK232-8 digested with the same enzymes. pKK232-8 was used as a negative control in all assays.

Plasmids pT3-EcpR-400 and pK3-EcpR-400 were constructed using primers ecpR-400F and Km-SstI-R (see Table S1 in the supplemental material) and DNA from EPEC *ecpR*::3×FLAG as the template (Table 1). The PCR products were digested with enzymes BamHI and SstI and cloned into plasmids pMPM-T3 and pMPM-K3 (Table 1), respectively, digested with the same enzymes.

Microplate CAT assays. The chloramphenicol acetyltransferase (CAT) assay and protein determinations to calculate specific activity were performed as described previously (44, 55). The strains used in this work to determine CAT activity of different *cat* transcriptional fusions did not

TABLE 1 Strains and plasmids used in this study

Strain or plasmid	Description	Reference or source
Strains		
E2348/69	Wild-type EPEC O127:H6	41
E2348/69 Δ*ecpR*::Km	E2348/69 carrying an in-frame deletion of *ecpR*	This study
E2348/69 EcpR-3×FLAG	E2348/69 *ecpR*::3×FLAG-Km	Martínez-Santos, unpublished
JPEP36	E2348/69 Δ*hns*::Km	García-Angulo et al., submitted
JPEP45	E2348/69 Δ*himA*::Km	García-Angulo et al., submitted
JPEP44	E2348/69 Δ*fis*::Km	García-Angulo et al., submitted
JPEP47	E2348/69 Δ*hha*::Km	García-Angulo et al., submitted
JPEP40	E2348/69 Δ*stpA*::Km	García-Angulo et al., submitted
EDL933	Wild-type EHEC O157:H7	60
EDL933 Δ*ecpR*	EDL933 carrying an in-frame deletion of *ecpR*	This study
EDL933 Δ*ecpA*::Km	EDL933 carrying an in-frame deletion of *ecpA*	57
EDL933 Δ*hns*::Km	EDL933 carrying an in-frame deletion of *hns*	This study
EDL933 Δ*himA*::Km	EDL933 carrying an in-frame deletion of *himA*	This study
MC4100	F′ *araD139* Δ(*argF-lac*)*U169 rpsL150 relA1 flb5301 deoC1 ptsF25 rbsR*	12
JPMC1	MC4100 derivative, Δ*hns*::*kan*	5
JPMC2	MC4100 derivative, Δ*himA*::*kan*	10
JPMC35	MC4100 derivative, Δ*hns* Δ*himA*::*kan*	10
DH5a	*supE44* Δ*lacU169* F80 *lacZ* ΔM15 *hsdR17 recA1 endA1 gyrA96 thi-1 relA1*	Invitrogen
Plasmids		
pKD46	λ Red recombinase system plasmid	17
pKD4	Km cassette template plasmid	17
pCP20	FLP recombinase plasmid	17
pMPM-T3	Low-copy-number cloning vector; p15A derivative; Tc^r	45
pT3-EcpR-400	pMPM-T3 derivative carrying *ecpR*::3×FLAG plus its regulatory region up to position −288 with respect to the TSS	This study
pT3-EcpR	pT3-EcpR-400 derivative carrying *ecpR*::3×FLAG plus its regulatory region up to position −59 with respect to the TSS	This study
pT3-EcpR-D60A	pT3-EcpR expressing EcpR D60A	This study
pT3-EcpR-G159A	pT3-EcpR expressing EcpR G159A	This study
pT3-EcpR-N170K-T175A	pT3-EcpR expressing EcpR T175A/N170K	This study
pT3-EcpR-T175A	pT3-EcpR expressing EcpR T175A	This study
pT3-EcpR-V176A	pT3-EcpR expressing EcpR V176A	This study
pT3-EcpR-V176A-Q196L	pT3-EcpR expressing EcpR V176A/Q196L	This study
pT3-EcpR-K186A	pT3-EcpR expressing EcpR K186A	This study
pMPM-K3	Low-copy-no. cloning vector; p15A derivative; Km^r	45
pK3-EcpR-400	pMPM-K3 derivative carrying *ecpR*::3×FLAG up to position −288 with respect to the TSS	This study
pBAD/Myc-His A	pBR322 derived-expression vector containing a C-terminal *myc* epitope tag and polyhistidine region	Invitrogen
pGTG	pBAD/Myc-His derivative expressing EcpR-MycHis	Martínez-Santos, unpublished
pKK232-8	pBR322 derivative containing a promoterless chloramphenicol acetyltransferase *cat* reporter gene	Pharmacia Biotech
pecpR-1H	*ecpR-cat* transcriptional fusion from position −591 to +198 from EHEC	This study[a]
pecpR-1P	*ecpR-cat* transcriptional fusion from position −590 to + 198 from EPEC	This study
pecpR-2	*ecpR-cat* transcriptional fusion from position −480 to +198	This study
pecpR-3	*ecpR-cat* transcriptional fusion from position −379 to +198	This study
pecpR-4	*ecpR-cat* transcriptional fusion from position −288 to +198	This study
pecpR-4m1	pecpR-4 with bases −212 to −208 changed from ATTCC to CGGAA	This study
pecpR-4m2	pecpR-4 with bases −194 to −191 changed from CAAA to ACCC	This study
pecpR-4m3	pecpR-4 with bases −198 to −187 changed from AGGGCAAAGTTC to CTTTACCCTGGA	This study
pecpR-4m4	pecpR-4 with bases −189 to −186 changed from TTCC to GGAA	This study
pecpR-4IRm1	pecpR-4 with bases −97, −96, −93, and −92 changed from CAAT to GGCC, respectively	This study
pecpR-4IRm2	pecpR-4 with bases −100 to −89 changed from AAGCAATATTTT to GGGGCGCACCGG	This study
pecpR-5	*ecpR-cat* transcriptional fusion from position −236 to +198	This study
pecpR-5 m	pecpR-5 with bases −220 to −213 changed from TTAAGACT to GGCCTCAG	This study
pecpR-6	*ecpR-cat* transcriptional fusion from position −211 to +198	This study
pecpR-7	*ecpR-cat* transcriptional fusion from position −199 to +198	This study
pecpR-8	*ecpR-cat* transcriptional fusion from position −188 to +198	This study
pecpR-9	*ecpR-cat* transcriptional fusion from position −103 to +198	This study
pecpR-10	*ecpR-cat* transcriptional fusion from position −66 to +198	This study
pecpR-11	*ecpR-cat* transcriptional fusion from position −38 to +198	This study
pecpR-12	*ecpR-cat* transcriptional fusion from position −6 to +198	This study
pecpR-13	*ecpR-cat* transcriptional fusion from position +26 to +198	This study
pecpR-14	*ecpR-cat* transcriptional fusion from position +75 to +198	This study
pecpA-270	*ecpA-cat* transcriptional fusion from position −270 to +22 with respect to the *ecpA* start codon.	This study
pecpA-180	*ecpA-cat* transcriptional fusion from position −180 to +22	This study
pecpA-80	*ecpA-cat* transcriptional fusion from position −80 to +22	This study
pecpRA-P	*ecpR-cat* transcriptional fusion from position −288 with respect to the TSS of *ecp*, to +22 with respect to the start codon of *ecpA* from EPEC	This study
pecpRA-H	*ecpR-cat* transcriptional fusion from position −288 with respect to the TSS, to +22 with respect to the start codon of *ecpA* from EHEC	This study

[a] Positions spanning the fragments contained in the transcriptional fusions are with respect to the transcriptional start site (TSS).

render measurable levels of CAT when carrying the empty vector pKK232-8 (data not shown).

Flow cytometry. Flow cytometry (FC) was used to detect the production of ECP and was performed as described previously (31). Briefly, 10^6 bacteria grown overnight in DMEM were incubated with 2% formalin for 10 min. Formalin was removed by centrifugation and repeated washes with PBS. Formalin-treated cells were incubated with anti-ECP antibodies overnight at 4°C. Bacterial cells were then washed and incubated with goat anti-rabbit IgG Alexa Fluor 488 conjugated for 1 h at 4°C. The Alexa Fluor fluorescence emission was collected through a 30-nm band pass filter centered at 530 nm in which 50,000 events were measured. Bacteria were labeled with propidium iodide and detected through a 42-nm band pass centered at 585 nm. The samples were analyzed in a Becton Dickinson FACScan.

Western immunoblotting. Overnight LB bacterial cultures of wild-type EHEC EDL933, or wild-type EPEC E2348/69 and their mutant derivatives in different regulatory genes, were subcultured into DMEM and incubated at room temperature under static growth conditions up to an OD_{600} of 1.0. Three milliliters of each bacterial suspension was pelleted and resuspended in 200 μl 1× PBS. Then samples were sonicated for 3 min, 60 μl of Laemmli buffer was added, and the mixture was boiled for 5 min. The samples were then subjected to SDS-PAGE (12% polyacrylamide) and transferred to 0.22-μm-pore-size nitrocellulose membranes (Amersham, United Kingdom). Membranes were blocked with 5% nonfat milk and incubated with antibodies against ECP (43), FLAG, Myc and DnaK (Invitrogen) (diluted 1:15,000, 1:5,000, 1:5,000 and 1:10,000, respectively). Membranes were washed with phosphate-buffered saline (PBS)−0.3% Tween 20, immunostained with a 1:10,000 dilution of horseradish peroxidase-conjugated goat anti-rabbit or anti-mouse antibodies (Biomeda), and developed with Western Lightning Plus-ECL chemiluminescence reagents (Perkin Elmer) according to the manufacturer's instructions. Bands were detected with X-ray film.

Site-directed PCR mutagenesis. Oligonucleotide site-directed mutagenesis to replace selected *ecpR* codons for alanine codons was performed using the QuikChange kit (Stratagene). Reactions were performed using plasmid pT3-EcpR-400 as the template (Table 1). The secondary mutations N170K and Q196L in the two double mutants were randomly obtained while generating single mutants with residues T175 and V176, respectively. To prevent the autoregulatory effect of wild-type EcpR and functional EcpR mutants, the regulatory region containing the EcpR-binding sites from pT3-EcpR-400, and from the resulting plasmids carrying mutated *ecpR* genes, was removed by digesting their DNA with EcoRI and religation, generating the pT3-EcpR series (Table 1). All the constructs were verified by DNA sequencing.

***In vivo* footprinting.** Footprinting of the *ecpR* regulatory region was performed *in vivo* using a system of two compatible plasmids as previously described (48), with slight modifications. EHEC EDL933 Δ*ecpR* carrying plasmid pecpR-4 or pecpR-4m2, plus either the empty vector pMPM-T3 or its derivative pT3-EcpR or pT3-EcpR-K186A (expressing wild-type EcpR or the EcpR K186A mutant, respectively), was grown in 5-ml shaken LB cultures at 37°C overnight. The strains were subcultured into 10 ml of DMEM and grown for 6 h at 37°C with shaking. Culture samples were collected, to which freshly prepared dimethyl sulfate (DMS) at a final concentration of 0.1% (vol/vol) was added for 1 min. Then the cultures were centrifuged at 12,000 rpm for 5 min at 4°C, and the pellet was washed twice with ice-cold saline phosphate solution (150 mM NaCl, 40 mM K_2HPO_4, 22 mM KH_2PO_4 [pH 7.2]). Methylated plasmid DNA was isolated using a High Pure Plasmid Isolation Kit (Roche Applied Science), according to the manufacturer's instructions, and it was eluted in 50 μl of water. Plasmid DNA was cleaved at the methylated positions by adding 5 μl of 1 M piperidine and incubating it at 90°C for 30 min, and then the DNA was precipitated with butanol, washed extensively with 70% ethanol, and finally dissolved in 100 μl of H_2O. Primer extension reactions were performed using [γ-^{32}P]ATP 5′-labeled oligonucleotides pKK-8-BHI and ecpR-3R (see Table S1 in the supplemental material), complementary to the pKK232-8 plasmid and the regulatory region of *ecp*, respectively, which were mixed with approximately 2 μg of methylated DNA in a final volume of 30 μl of TM buffer (10 mM $MgCl_2$, 10 mM Tris-HCl [pH 8.0]). Annealing was carried out by boiling the above mixture for 3 min and then immediately placing it into ice. Primers were extended with 1 U of the Klenow fragment of DNA polymerase I (Roche Applied Science) plus 0.1 mM each deoxynucleotide triphosphate for 10 min at 50°C. The extension products were precipitated, dried, suspended in loading buffer, and separated by gel electrophoresis on 7% polyacrylamide gels containing 8 M urea together with a sequence ladder using the same primers. The gel was dried and exposed to Kodak X-Omat film for 1 to 3 days.

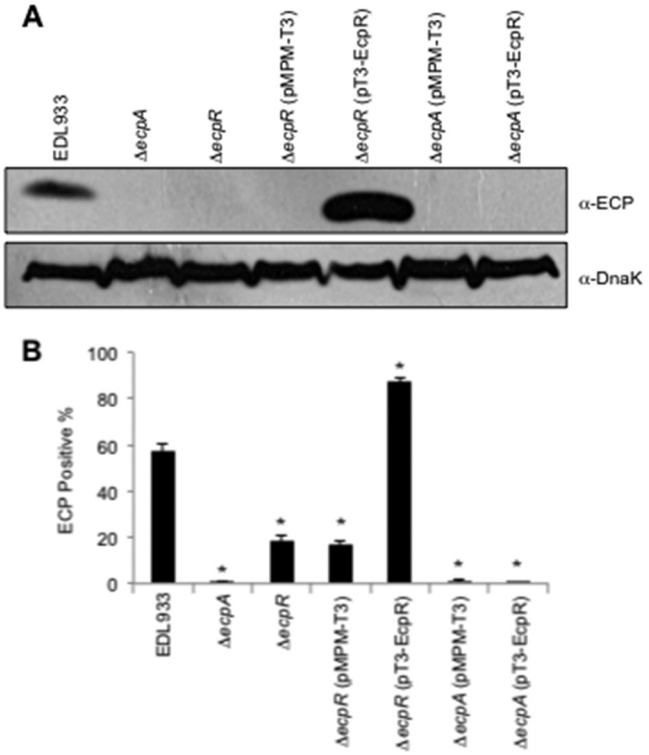

FIG 1 EcpR is required for the synthesis of ECP. (A) Western blot analysis of whole-cell extracts of EHEC EDL933 wild type, Δ*ecpA*, Δ*ecpR*, Δ*ecpR*/pMPM-T3, Δ*ecpR*/pT3-EcpR, Δ*ecpA*/pMPM-T3, and Δ*ecpA*/pT3-EcpR (Table 1) grown in DMEM at 30°C in static cultures. DnaK was detected as a loading control. (B) Production of ECP by wild-type EHEC and its isogenic *ecpA* and *ecpR* mutants, analyzed by flow cytometry using anti-ECP antibodies and goat anti-rabbit IgG Alexa Fluor 488 conjugate; 10,000 events were measured. Bacteria were recovered from the supernatant of HeLa cells infected for 6 h at 37°C. Error bars represent the standard deviations of three independent assays done in duplicate. *, $P < 0.02$ between wild-type and mutant strains, calculated using the unpaired Student *t* test.

RESULTS

EcpR acts as a positive regulator. The *ecp* or *mat* cluster comprises 6 genes named *ecpRABCDE* (also known as *matABCDEF*) (Fig. 3A). This operon was first described in NMEC as encoding meningitis-associated and temperature-regulated (Mat) fimbriae because it is mainly expressed at 20°C (38, 53). However, it was later shown to be conserved in, and expressed by, all *E. coli* pathotypes, not only NMEC, as well as by commensal *E. coli* strains, even at 37°C, and thus, the name *E. coli* common pilus (ECP) was proposed as an alternative to Mat to appropriately describe its ubiquitousness in *E. coli* (3, 6, 29, 57, 61, 63). This cluster seems to

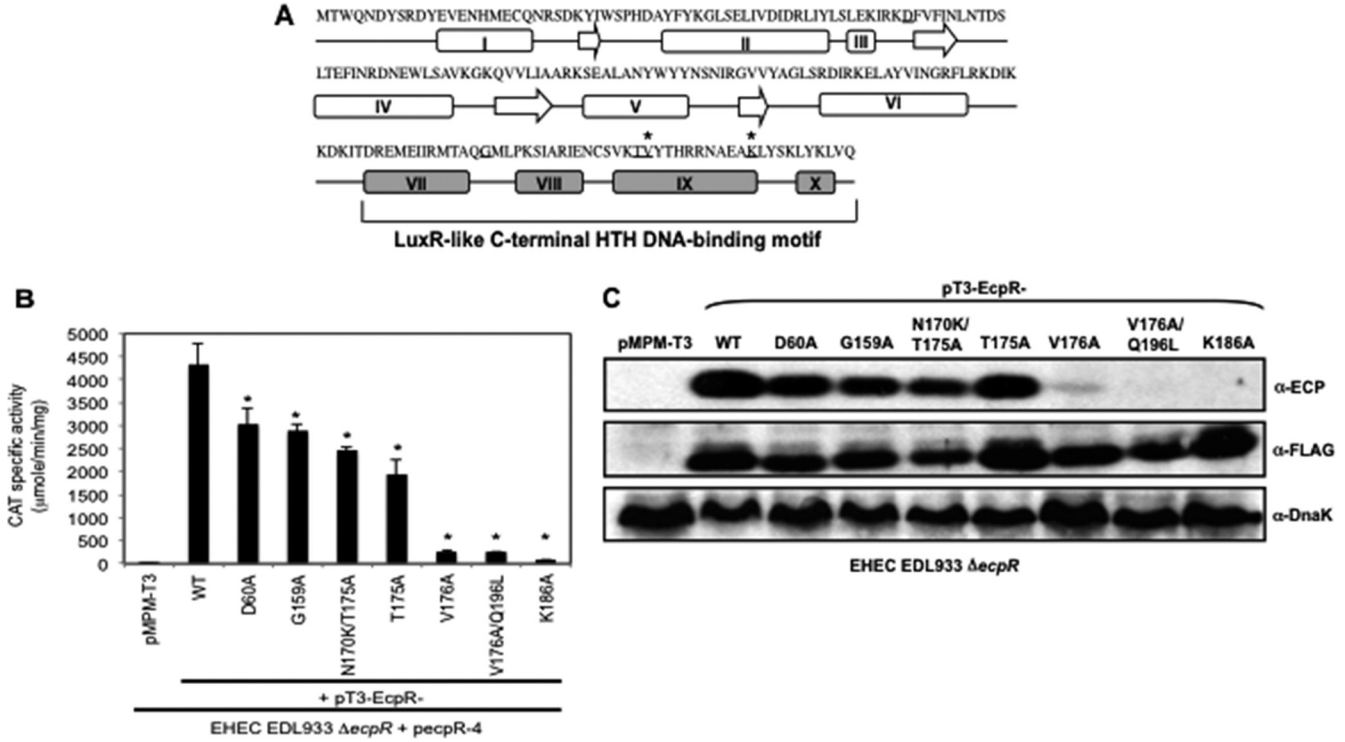

FIG 2 Mutations in the predicted HTH DNA-binding domain of EcpR affect its function. (A) Schematic representation of the predicted secondary structure of EcpR using the PSIPRED server. The arrows indicate β strands, and the rectangles represent α helices. Amino acids replaced by alanine are underlined. The asterisks indicate residues that affect EcpR activity when replaced by alanines. Helices VII, VIII, IX, and X corresponding to the putative EcpR HTH DNA-binding domain are shown in gray. (B) CAT activity assay with EDL933 Δ*ecpR* containing fusion ecpR-4 complemented with vector pMPM-T3 or plasmids encoding wild-type EcpR (pT3-EcpR) or the EcpR mutants (pT3-EcpR-D60A, pT3-EcpR-G159A, pT3-EcpR-N170KT175A, pT3-EcpR-T175A, pT3-EcpR-V176A, pT3-EcpR-V176AQ196L, and pT3-EcpR-K186A). The resulting strains were grown in DMEM at 37°C with shaking for 6 h. Error bars represent the standard deviations of the activity of three independent assays done in duplicate. *, $P < 0.0001$ between mutants and wild-type EcpR. (C) Western blot of whole-cell extracts of EHEC Δ*ecpR* transformed with vector pMPM-T3 or with plasmids encoding wild-type EcpR or the mutants. EcpR was detected with α-FLAG antibodies. DnaK was detected as a loading control.

share the standard genetic organization of the majority of the fimbrial gene clusters present in *E. coli* and *Salmonella* (30, 47). The second gene of the cluster codes for the 21-kDa main structural fimbrial subunit EcpA. Genes encoding a putative chaperone (*ecpB*) and usher (*ecpC*) make up the middle of the cluster. At the end are *ecpD* and *ecpE*, both of which share homology to genes encoding putative fimbrial proteins of *Proteus mirabilis* (data not shown). EcpD is a tip adhesin capable of assembling into thin filaments in the absence of EcpA (26) and EcpE is a potential chaperone.

The first gene of the cluster codes for EcpR, a 196-amino-acid (aa) protein predicted to possess an HTH DNA-binding motif (Fig. 2A) that has similarity to regulatory proteins from the LuxR/FixJ family (see Fig. S1 in the supplemental material). Proteins from this family have been shown to act as classic activators or repressors (reviewed in reference 50). To provide clues regarding the potential role of EcpR in *ecp* regulation, we analyzed by Western blotting the production of EcpA in bacterial cell extracts from wild-type EHEC strain EDL933 and its Δ*ecpR* and Δ*ecpA* mutant derivatives, or the mutants carrying the empty vector pMPM-T3 or a plasmid coding for EcpR (pT3-EcpR) (Fig. 1A and Table 1). There is no EcpA production in the *ecpA* mutant alone or carrying either plasmid. The production of EcpA was reduced in the *ecpR* mutant alone or carrying vector pMPM-T3, while it was enhanced above the production detected in the wild-type strain when the mutant was complemented with pT3-EcpR. Similar observations were obtained by flow cytometry (Fig. 1B). In the *ecpR* mutant the production of ECP was reduced about 66%, and when complemented with plasmid pT3-EcpR, the production of ECP increased about 50% with respect to that of the wild-type strain. Together these results show that EcpR has a positive effect on the production of the ECP proteins.

Point mutations in the C terminus of EcpR affect its function. In order to further evaluate the transcriptional activator nature of EcpR and the role of its putative HTH DNA-binding domain, alanine substitutions of residues D60, G159, T175, V176 and K186 (Fig. 2A), which include some of the most conserved residues at the HTH domain of well-characterized proteins of the LuxR family, such as NarL, UhpA, FixJ, GerE, MalT and LuxR (see Fig. S1 in the supplemental material), were generated. The resulting plasmids, pT3-EcpR-D60A, -G159A, -T175A, -V176A, and -K186A, as well as the spontaneous double mutants pT3-EcpR-N170K-T175A and -V176A-Q196L (Table 1), were tested for their ability to activate the pecpR-4 fusion (Table 1) in the EHEC Δ*ecpR* mutant (Fig. 2B). The EcpR D60A, G159A, and TI75A mutants, as well as the N170K/T175A double mutant, showed only a modest reduction in their activation capacity compared to the wild-type protein. In contrast, the EcpR V176A, V176A/Q196L, and K186A mutants were unable to activate the pecpR-4 fusion. The phenotype of these mutants was further analyzed by testing their capac-

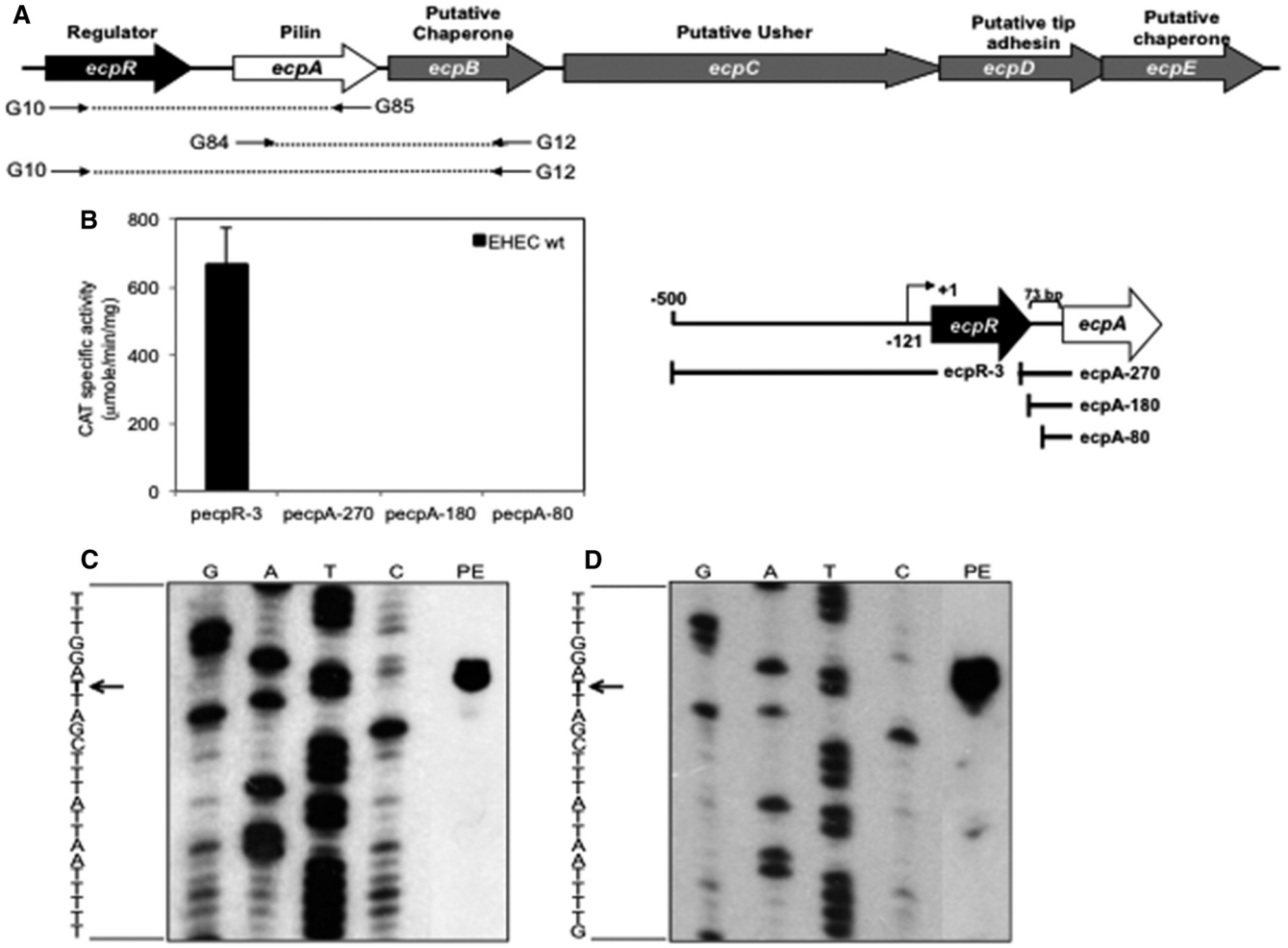

FIG 3 The *ecpRABCDE* genes are transcribed as an operon. (A) Schematic representation of the *ecp* cluster formed by genes *ecpR* and *ecpA* to *ecpE*. The putative function of each gene is indicated above the big arrows. The arrows below the schematic represent the primers used for RT-PCR, and the dashed lines represent the products obtained with each pair of primers. (B) CAT activity produced by EHEC EDL933 transformed with fusions ecpR-3, ecpA-270, ecpA-180, and ecpA-80 (left panel). Error bars indicate standard deviations of results from three independent experiments with duplicates. The right panel is the schematic representation of the *ecpR* and *ecpA-cat* transcriptional fusions used in the left panel. The broken arrow indicates the transcriptional start site. The *ecpA* gene is separated from *ecpR* by 73 bp. As a negative control, the strain transformed with vector pKK232-8 was used. (C and D) Identification of the transcriptional start site. Total RNA from the wild-type EHEC strain EDL933 (C) and EPEC E2348/69 (D) transformed with fusions ecpRA-H and ecpRA-P, respectively, was extracted from DMEM culture samples collected at an OD_{600} of 1.0. A primer specific for the 5′ end of the coding region of *ecpR* (positions +136 to +156, with respect to the transcriptional start site) and 10 μg of total RNA were used for the primer extension reaction, as indicated in Materials and Methods. The arrows indicate the bases corresponding to the transcriptional start sites.

ity to activate the production of EcpA by Western blotting (Fig. 2C). The mutants that activated the expression of pecpR-4 were also able to complement EcpA synthesis in EHEC Δ*ecpR*, but not those mutants that showed a defect activating the fusion (Fig. 2B and C). These results indicated that the conserved residues V176 and K186 are essential for the activity of EcpR and suggested that the HTH domain is likely involved in protein-DNA interactions. The lack of function of the three inactive EcpR mutants was not due to the lack of expression, since the FLAG epitope was detected at similar levels in the wild-type and mutants, as seen by Western blotting using an anti-FLAG antibody (Fig. 2C).

The *ecp* cluster is transcribed as an operon from a promoter located upstream of *ecpR*. In order to determine whether *ecpR* is transcribed with the rest of the genes in the cluster, we performed RT-PCR experiments using primers derived from the beginning or the end of *ecpR*, *ecpA* and *ecpB* (Fig. 3A). We were able to detect mRNA for *ecpR*, *ecpA*, and *ecpB* (data not shown), indicating that at least these three genes are transcribed as an operon and that transcription is initiated upstream of *ecpR*. Since *ecpA* codes for the structural subunit of ECP, we then explored the possibility that, in addition to being transcribed from the *ecpR* promoter, the *ecpA* gene could also be expressed from an internal promoter driving the expression of the genes involved in ECP biogenesis. With this purpose, we constructed three transcriptional fusions containing different portions of the *ecpR-ecpA* intergenic region and a fusion carrying the putative upstream regulatory region of *ecpR* to the promoterless chloramphenicol acetyltransferase (*cat*) gene, as described in Materials and Methods. The resulting fusions, ecpA-270, ecpA-180 and ecpA-80 (Fig. 3B, right panel), were inactive when tested in EHEC EDL933 (Fig. 3B, left panel), while a fusion containing the *ecpR* upstream region (ecpR-3) was active. This result further supported the notion

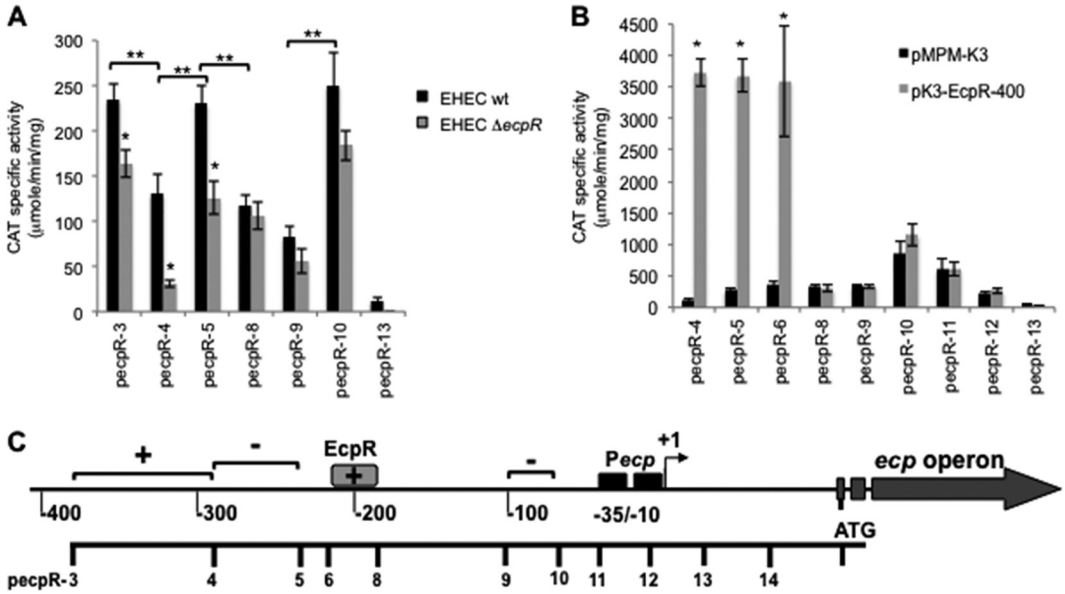

FIG 4 Identification of regulatory elements involved in *ecp* regulation. (A) Expression of *cat* transcriptional fusions contained in plasmids ecpR-3, ecpR-4, ecpR-5, ecpR-8, ecpR-9, ecpR-10, and ecpR-13 in wild-type EHEC EDL933 and its Δ*ecpR* isogenic mutant. (B) Expression of *cat* transcriptional fusions contained in plasmids ecpR-4, ecpR-5, ecpR-6, ecpR-8, ecpR-9, ecpR-10, ecpR-11, ecpR-12, and ecpR-13 in EHEC Δ*ecpR* also carrying vector pMPM-K3 or plasmid pK3-EcpR-400. CAT-specific activity was determined from samples obtained from static DMEM cultures grown at 30°C. Error bars represent the standard deviations of the activity of three independent assays done in duplicate. *, $P < 0.0001$ between gray and black bars in panels A and B. **, $P < 0.0001$ between black bars in panel A. (C) Schematic representation of the regulatory region of *ecp*. The broken arrow indicates the transcriptional start site, and the black boxes represent the −10 and −35 boxes. Brackets represent positive (+) and negative (−) regulatory elements. The gray box spans the proposed EcpR-binding site according to the deletion analysis. The scale below the schematic indicates the 5′ end of each fusion.

that the *ecp* cluster is transcribed from a promoter located upstream of *ecpR*.

In order to identify its promoter and to begin a detailed analysis of the regulatory region of the *ecp* operon, we performed primer extension experiments using RNA samples obtained from EHEC strain EDL933 and EPEC strain E2348/69 carrying plasmids pecpRA-H and pecpRA-P, respectively. The results of these experiments revealed that the *ecp* transcriptional start site corresponds to two A residues located 121 and 120 nucleotides upstream of the start codon of EHEC and EPEC *ecpR* (Fig. 3C and D), respectively. The putative −35 (TTGACA) and −10 (ATAAAT) boxes are separated by 17 nucleotides and contain six and three (underlined) out of six bases that are present in the consensus −35 and −10 sequences, respectively (Fig. 5A), of sigma 70-dependent promoters in *E. coli*.

Identification of *cis*-acting regulatory elements. The regulatory region of *ecp* is 99% identical between EPEC E2348/69 and EHEC EDL933, having just a few differences that may not affect expression. To evaluate this possibility, we compared the activities of both the EHEC (ecpR-1H) and EPEC (ecpR-1P) *ecpR-cat* fusions. The levels of activity of these fusions were similar when tested in both EPEC and EHEC (data not shown), indicating that the few changes between the *ecp* regulatory sequences of EPEC and EHEC do not modify their expression. Then, in order to identify regulatory elements involved in the transcriptional regulation of the *ecp* operon, we constructed several *cat* transcriptional fusions spanning different fragments of the regulatory region of *ecp* (Table 1; Fig. 4C). All fusions contained a common 3′ end at position +198 with respect to the transcriptional start site and serial eliminations of DNA sequences of the regulatory region from the 5′ end. These fusions were introduced into EHEC EDL933, and CAT activity was determined under growth conditions that enhance ECP expression (DMEM cultures at 30°C) (Fig. 4A). Fusion ecpR-3 showed an activity similar to that seen for ecpR-1H and ecpR-2 in wild-type EHEC (data not shown), while the ecpR-4 fusion showed an activity approximately 44% lower, suggesting that there is a positive regulatory element between positions −379 and −288. The ecpR-5 fusion showed an activity similar to that of fusion ecpR-3, suggesting that there is a negative regulatory region between positions −288 and −236. Fusions ecpR-8 and ecpR-9 had an activity of 50 and 64%, respectively, lower than that of fusion ecpR-5, suggesting the presence of a positive regulatory element between positions −236 and −188, while fusion ecpR-10 showed almost three times the activity of fusion ecpR-9, suggesting that a negative regulatory element exists between positions −103 and −66 (Fig. 4A and C). The ecpR-13 fusion showed background levels of activity that were consistent with the fact that it does not contain the putative promoter. These analyses allowed us to get insights into the distribution of regulatory elements at the upstream region of *ecpR* that are involved in both positive and negative regulation of *ecp*.

EcpR acts at the transcriptional level. As described above, EcpR has a positive influence on the expression of the *ecp* promoter. To further characterize the role of EcpR as a positive regulator of *ecp*, we tested the *ecpR-cat* transcriptional fusions in an EHEC Δ*ecpR* strain (Fig. 4A, gray bars). The activity of the ecpR-3 fusion in the mutant strain was slightly reduced (approximately 30%) with respect to the activity seen in wild-type EHEC; however, the activity of fusions ecpR-4 and ecpR-5 was reduced (~76% and 45%, respectively) in the absence of EcpR compared

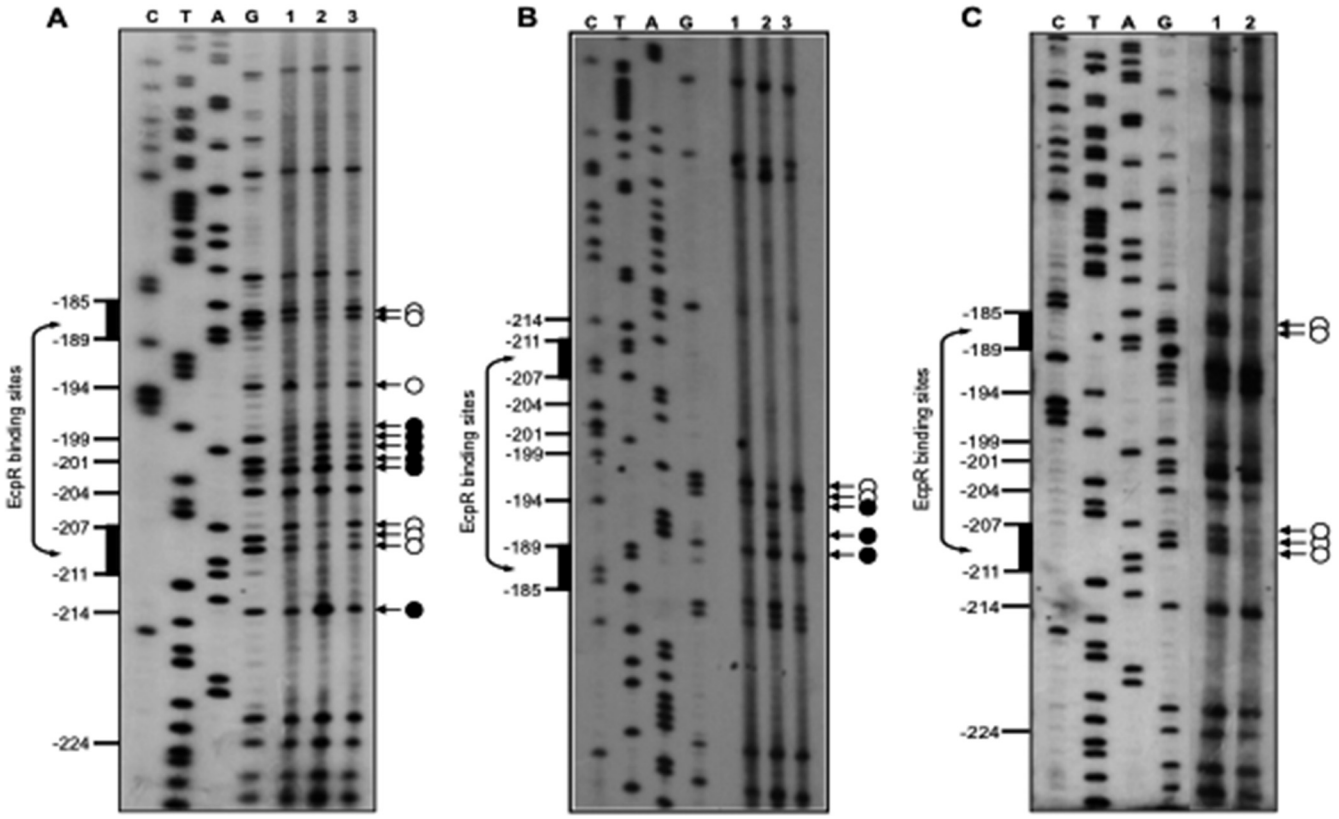

FIG 5 Identification of the EcpR-binding site. (A to C) *In vivo* DMS footprinting analysis of the EHEC *ecp* regulatory region. Bacterial cultures of EHEC EDL933 Δ*ecpR* containing fusion ecpR-4 (A and B) or ecpR-4m2 (C) plus either the empty vector pMPM-T3 (lanes 1) or plasmids expressing wild-type EcpR (pT3-EcpR, lanes 2) or the EcpR K186A inactive mutant (pT3-EcpR-K186A, lanes 3) were exposed to DMS, and the plasmid DNA was extracted and treated as described in Materials and Methods. Primer extension products were amplified with primers pKK-8-BHI (A and C) and ecpR-3R (B) and resolved by 7% polyacrylamide–8 M urea gel electrophoresis and visualized by autoradiography. White circles and black circles indicate protected and hypermethylated sites, respectively. Black vertical bars on the left side indicate the bases spanning the putative EcpR-binding sites. The sequencing ladder was obtained with the same primers.

to the wild-type strain. In contrast, the expression of fusions ecpR-8, ecpR-9 and ecpR-10 was not significantly different between the wild-type and Δ*ecpR* strains, suggesting that a putative sequence motif required for EcpR-mediated activation was located between positions −236 to −186 with respect to the transcriptional start site (Fig. 4A and C).

When the expression of representative transcriptional fusions was analyzed in the EHEC Δ*ecpR* strain carrying vector pMPM-K3 or plasmid pK3-EcpR-400 (expressing EcpR), a very dramatic increase in expression was observed for fusions ecpR-4 and ecpR-5 (between 33- and 13-fold), but not for the shorter fusions, whose activity was not altered by EcpR (Fig. 4B). This effect was also seen for ecpR-6 (Table 1), which was constructed to further delimit the sequence involved in EcpR-mediated activation. Taken together, these results indicate that EcpR positively regulates its own expression, and thus of all the *ecp* genes that are transcribed as an operon, by most likely interacting with a sequence motif located downstream of position −211.

EcpR binds to two small direct repeats distantly located with respect to the *ecp* promoter. The body of evidence above strongly supports a role of EcpR as a positive regulator. To further characterize the interaction of EcpR with the *ecp* regulatory region, we performed *in vivo* methylation interference footprinting experiments. Cultures of EHEC Δ*ecpR* carrying fusion ecpR-4 plus either the empty vector pMPM-T3 or plasmids expressing wild-type EcpR (pT3-EcpR) or the inactive mutant EcpR K186A (pT3-EcpR-K186A) carrying a mutation in the putative HTH DNA-binding domain (Fig. 2) were treated with DMS prior to plasmid DNA purification. Figure 5A shows the primer extension products of the *ecpR* regulatory region spanning the proposed EcpR-binding sequence at the bottom strand. Comparison of the intensities of the products showed that when wild-type EcpR is present (Fig. 5A, lane 2), residues at positions −186, −187, −194 and −207 to −209, with respect to the transcriptional start site, were protected from methylation. Other residues between positions −198 to −202 were hypermethylated when wild-type EcpR was present. In contrast, the EcpR K186A mutant (Fig. 5A, lane 3) did not change the methylation pattern of this sequence with respect to the control (Fig. 5A, lane 1). The methylation pattern at the top strand was also analyzed (Fig. 5B). In this case, changes in the methylation pattern were also seen in the presence of wild-type EcpR around the proposed binding sequence between positions −197 to −190 (lane 2) but not in the presence of the empty vector or the plasmid expressing the EcpR K186A mutant (lanes 1 and 3, respectively). Bases protected by EcpR are contained within two TTCCT direct repeats separated by a 17-bp spacer where several bases were hypermethylated in the presence of EcpR (Fig. 6A). To determine the role of these sequence elements in EcpR-mediated

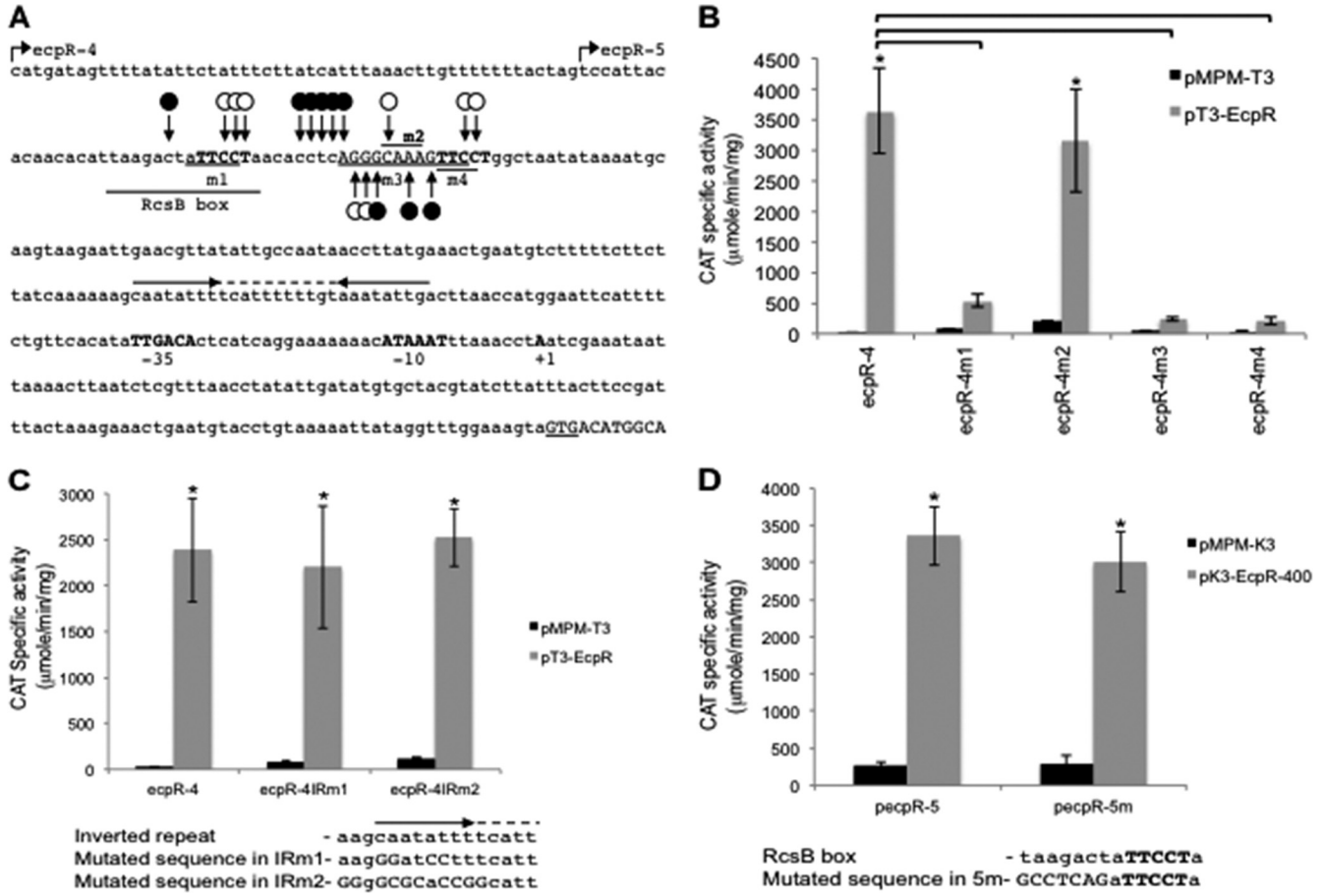

FIG 6 Analysis of *ecp* regulatory elements by site-directed mutagenesis. (A) Sequence of the regulatory region of *ecp*. The EcpR start codon (GTG) is underlined. The transcriptional start site, the −10 and −35 hexamers, and the putative binding sites for EcpR, corresponding to the TTCCT boxes, are indicated in bold uppercase letters. The bases changed in mutants ecpR-4m1 to ecpR-4m4 are underlined, as well as the RcsB box. The broken arrows represent the 5′ limit of the ecpR-4 and ecpR-5 fusions at positions −288 and −236, respectively. Black circles represent the hypermethylated bases observed by *in vivo* footprinting, while white circles represent protected bases. The horizontal arrows indicate the locations of an inverted repeat, and the dashed line indicates the 11-bp spacer. (B) Analysis of the TTCCT boxes. CAT activity of fusions ecpR-4, ecpR-4m1, ecpR-4m2, ecpR-4m3, and ecpR-4m4. Changes in each mutant fusion are indicated in panel A. (C) Analysis of the inverted repeats. CAT activity of fusions ecpR-4, ecpR-4IRm1 and ecpR4IRm2. The wild-type and mutant sequences of the region spanning the left arm of the inverted repeat are shown below. (D) Analysis of the RcsB box. CAT activity of fusions pecpR-5 and pecpR-5m. The wild-type and mutant sequences of the RcsB box are shown below. The bases changed in fusion pecpR-5m are indicated with capital letters. CAT activity was determined from culture samples of EHEC EDL933 Δ*ecpR* complemented with the empty vector pMPM-T3 (B and C) or pMPM-K3 (D) or plasmid pT3-EcpR (B and C) or pK3-EcpR-400 (D) plus the different transcriptional fusions. The activity is the result of three independent experiments done in duplicate. Asterisks (*) correspond to *P* values of <0.0001 between gray and black bars. Brackets correspond to *P* values of <0.0001 between gray bars.

activation, mutant fusions ecpR-4m1 to ecpR-4m4 were generated (Fig. 6A and Table 1) and their activities tested in the presence of EcpR (Fig. 6B). Interestingly, fusions containing changes that modified the TTCCT boxes (ecpR-4m1, ecpR-4m3, and ecpR-4m4) no longer responded to EcpR, while changes in the spacer region between the two TTCCT boxes (ecpR-4m2) (Fig. 6B), in an inverted repeat located between the proximal TTCCT box and the promoter (ecpR-4IRm1 and ecpR-4IRm2) (Fig. 6C) or in the sequence right upstream of the distal TTCCT box (ecpR-5m) (Fig. 6D), corresponding to the first half of the recently reported RcsB-binding sequence in the *ecp* operon of meningitis *E. coli* (40), did not affect EcpR-mediated activation.

These results suggested that upon EcpR binding to the TTCCT boxes, which are protected from methylation, the topology of the spacer sequence, which does not seem to be required for EcpR binding, is altered, exposing it to hypermethylation. Consistent with this notion, the spacer sequence of fusion ecpR-4m2 containing four changes was also hypermethylated without affecting EcpR binding to the TTCCT boxes (Fig. 5C) or its activation by EcpR (Fig. 6B). Our finely tuned mapping approach revealed that the putative EcpR-binding sites are distantly located from the promoter between positions −211 and −185, at a noncanonical distance for LuxR-like regulators.

IHF counteracts the repression exerted by H-NS and is essential for EcpR activity. The regulation of fimbrial operons often involves, in addition to the elements encoded within the operon, global regulators such as IHF and H-NS (14). In order to determine if global regulators were also involved in *ecp* activation, we analyzed the activity of fusion ecpR-1 in EPEC E2348/69 and its Δ*hns*, Δ*fis*, Δ*hha*, Δ*himA*, and Δ*stpA* derivative mutant strains (Table 1). No difference was observed between the wild-type strain and the Δ*fis*, Δ*hha*, and Δ*stpA* mutants (see Fig. S2A in the

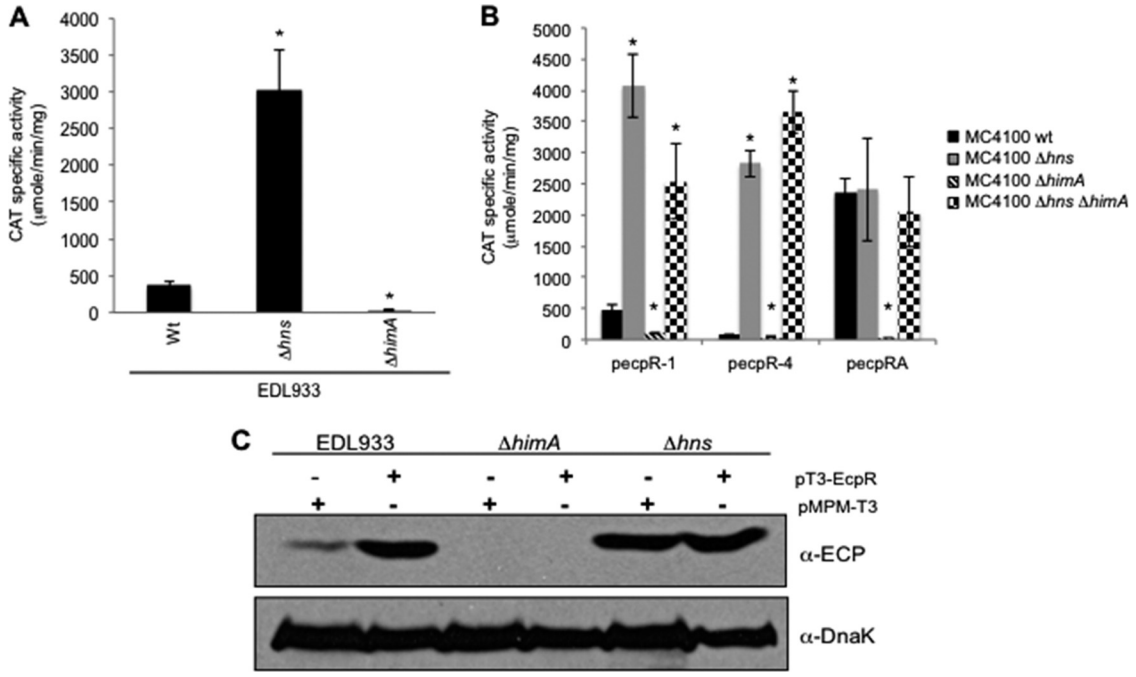

FIG 7 Global regulators IHF and H-NS regulate *ecp* expression. (A) CAT activities of fusion ecpR-1 in wild-type EHEC EDL933 and its Δ*hns* and Δ*himA* isogenic mutants. *, *P* values of <0.0001. (B) CAT activity assay with *E. coli* K-12 strain MC4100 and its Δ*hns*, Δ*himA*, and Δ*himA* Δ*hns* isogenic mutants transformed with fusions ecpR-1, ecpR-4, and ecpRA. Error bars indicate standard deviations of results from three independent experiments with duplicates. *, *P* values of <0.0001 between wild-type and mutant strains, calculated using the unpaired Student *t* test. (C) Western blot with the anti-ECP antibody of whole-cell extracts of EHEC EDL933 and its Δ*hns* and Δ*himA* isogenic mutants transformed with vector pMPM-T3 or plasmid pT3-EcpR (Table 1). DnaK was detected as a loading control using a monoclonal anti-DnaK antibody.

supplemental material). In contrast, in the Δ*hns* and Δ*himA* mutants, a significant increase and reduction, respectively, in *ecp* promoter activation was observed, indicating that H-NS and IHF regulate negatively and positively, respectively, the expression of the *ecp* promoter (Fig. S2A). These results were further confirmed in EHEC EDL933 and its Δ*hns* and Δ*himA* isogenic mutants (Table 1). A 7-fold increase in activity was observed in the *hns* mutant, while in the Δ*himA* strain the activity was 16 times lower than in the wild-type strain (Fig. 7A).

In order to confirm the role of IHF and to determine if EcpR is acting in synergy with it to regulate the expression of the *ecp* operon, we analyzed the level of EcpA production by Western blotting using whole-cell extracts of wild-type EHEC EDL933 and its Δ*hns* and Δ*himA* mutants transformed with the empty vector pMPM-T3 or with plasmid pT3-EcpR expressing EcpR (Fig. 7C). As expected, an increase in EcpA production in EHEC/pT3-EcpR (lane 2) was observed compared to EHEC/pMPM-T3 (lane 1). In the Δ*himA* mutant the production of EcpA was abolished, whether transformed with the empty vector or plasmid pT3-EcpR (lanes 3 and 4, respectively), indicating that IHF is essential for the EcpR-dependent activation of the *ecp* promoter. In contrast, in the *hns* mutant similar production of EcpA was detected, regardless of the presence of the vector or the pT3-EcpR plasmid (lanes 5 and 6, respectively), confirming the role of H-NS as a repressor of *ecp* expression. The same expression pattern was seen in EPEC and its Δ*himA* and Δ*hns* mutant derivatives (Fig. S2B).

To get insights into the mechanism by which IHF positively regulates the expression of *ecp,* fusions ecpR-1, ecpR-4, and ecpRA were transformed into the wild-type *E. coli* K-12 strain MC4100 and its Δ*hns*, Δ*himA* and Δ*himA*/Δ*hns* mutants (Table 1), which we have previously shown are a suitable host to use to study the interplay between H-NS and IHF in the transcriptional regulation of EPEC virulence genes (10). This strain lacks the *ecp* operon, as seen by PCR with primers specific for *ecpR* and *ecpA* (data not shown). The expression of fusions ecpR-1 and ecpR-4 increased approximately 8 and 36 times, respectively, in the *hns* mutant (Fig. 7B), similar to what was observed in EHEC and EPEC (Fig. 7A and see Fig. S2A in the supplemental material, respectively). However, in the *himA* mutant, the expression of these fusions decreased to background levels, as seen in EHEC and EPEC Δ*himA* strains (Fig. 7A and S2A, respectively). In contrast, the activities of both fusions in the *himA hns* double mutant were similar to the activities obtained in the *hns* single mutant, suggesting that the function of IHF is to regulate positively the expression of the *ecp* operon by counteracting the repression exerted by H-NS. On the other hand, the ecpRA fusion, which contains the *ecpR* gene and thus expresses EcpR, showed an activity in the wild-type strain approximately 30 times higher than the activity of the ecpR-4 fusion (both fusions contain up to position −288 of the *ecpR* regulatory region with respect to the transcriptional start site), further confirming the role of EcpR as a positive regulator. The activity obtained in the *hns* mutant was similar to that obtained in the wild-type strain, suggesting that the role of EcpR is also to counteract, with the aid of IHF, the repression exerted by H-NS. In contrast, the activity in the *himA* mutant was completely abolished, further supporting that IHF is essential for the EcpR-mediated activation of the *ecp* promoter; however, in the *himA hns* double mutant the fusion's activity was similar to that obtained in the wild-type and Δ*hns*

strains, indicating that when H-NS is absent, both IHF and EcpR are no longer required.

DISCUSSION

The regulation of ECP is just starting to be elucidated. The aim of this work was to analyze the transcriptional regulation of the *ecp* operon, as well as to study the role of EcpR, the product of the first gene. Analogous to other pilus systems, we found that the genes constituting the *ecp* cluster are transcribed as an operon and that EcpR is a positive regulator resembling the organization of other fimbrial operons, in which the first gene encodes a protein involved in their transcriptional regulation. For example, the *pap* operon, in which the *papB* regulator is transcribed along with the *papA* pilin (4), although there is no similarity between the pilin subunits or the regulators.

EcpR, also known as MatA, belongs to the superfamily of proteins containing a LuxR_C-like DNA-binding HTH domain (2). Many members of this family are canonical response regulators activated by sensor histidine kinases (e.g., members of the NarL/FixJ subfamily) (25), but others respond to different regulatory molecules. In these cases, the N-terminal domain modulates the activity of the C-terminal domain by means of several modifications in response to different environmental cues. For example, some proteins, like LuxR of *Vibrio fischeri*, bind quorum-sensing signaling molecules on their N-terminal domain (28); others, like *E. coli* NarL (21) and *Sinorhizobium meliloti* FixJ (1, 58), are phosphorylated at a conserved Asp residue; *E. coli* MalT binds maltotriose (56) and ATP (59); and GerE is the smallest member of the family lacking an N-terminal domain (20). Interestingly, the N terminus of EcpR does not share similitude with any of these proteins, nor contains any conserved functional domains, and thus represents a novel member of this protein family.

Despite the conservation of several C-terminal amino acid residues with response regulators of the NarL/FixJ subfamily and of a putative phosphoacceptor aspartic acid residue (D60), EcpR lacks most of the key N-terminal residues of the active site of canonical receiver domains. In agreement with this observation, the EcpR D60A mutant was not affected in its ability to activate the expression of the *ecp* promoter or to induce the synthesis of EcpA (Fig. 2). In contrast, the corresponding residue in the nitrate response regulator NarL (D59) was shown to be essential for its activity (21).

It has been shown for LuxR that truncated versions of the protein containing the HTH domain, but not the autoinducer-binding domain, are still active and no longer autoinducer dependent (13), this being the reason why it has been proposed that the N terminus interferes with the DNA-binding activity of the HTH domain in the absence of the inducer. In the case of EcpR, we constructed three truncated versions of the protein (named EcpR ΔN85, ΔN110, and ΔN129); however, none of them was able to complement *ecp* activation (data not shown), suggesting that EcpR, in contrast to LuxR, does not possess a modular structure and has to be intact to be functional.

The predicted HTH domain of EcpR is most likely involved in DNA binding, since two mutants, EcpR V176A and K186A, carrying alanine substitutions in two highly conserved residues at the putative recognition helix, were inactive. Furthermore, the K186A mutant was shown by *in vivo* footprinting to be unable to occupy the EcpR putative binding boxes that were shown by deletion and site-directed mutagenesis to be essential for the EcpR-dependent activation of the *ecp* promoter. In agreement with this observation, a mutation of the corresponding K198 residue in NarL also generated a defective mutant (42). Interestingly, the EcpR T175A mutant did not have a phenotype even when this residue was also highly conserved in the recognition helix of different LuxR-like regulators, suggesting that slight modifications in this helix may determine specificity for its unique binding sequence. However, at least for GerE of *Bacillus subtilis*, this residue has been shown to be important for transcriptional activation (15).

Representative members of this family have been shown to form dimers and to interact with inverted repeat sequences of different lengths. Such is the case for EsaR from *Pantoea stewartii* (46) and ExpR from *Erwinia chrysanthemi* (49), among others. LuxR family regulators may share a similar organization of their target binding sites (72). For example, LuxR dimers bind the *lux* box, a 20-bp inverted repeat (67), TraR binds to a 18-bp inverted repeat (75), GerE dimers bind two 12-bp consensus sequences in an inverted orientation with the central four bases overlapping (15, 20), and the NarL dimer binds two 7-bp inverted repeats separated by 2 bp (16). In contrast, EcpR seems to bind to two 5-bp direct repeats, the TTCCT boxes, separated by 17 bp, which are located between positions −211 and −185 with respect to the transcriptional start site at a noncanonical distance from the *ecp* promoter. Each TTCCT box is individually essential for the EcpR-mediated activation of the *ecp* promoter, suggesting that EcpR may bind to them as a dimer.

Furthermore, the distant location of the putative EcpR target TTCCT boxes upstream of position −185 suggested that EcpR might require additional regulatory elements to influence the activation of the *ecp* promoter. In agreement with this notion, the global heterodimeric regulator IHF was identified as an essential element for the activation of the *ecp* promoter, suggesting that it is required to generate the appropriate structural changes (e.g., by DNA looping) at the *ecp* regulatory region to facilitate the interaction of EcpR with the promoter and/or to disrupt or prevent the formation of repressor complexes by H-NS, which was found to strongly repress *ecp* expression. Global regulators such as IHF and H-NS have been shown to be involved in the transcriptional regulation of different fimbrial operons, which are also regulated by specific regulatory proteins belonging to different protein families (14).

Although the interplay between H-NS, IHF and the LuxR_C-like protein EcpR seems to represent a novel scheme in fimbrial regulation, some models of the complex interaction between members of the LuxR_C-like superfamily and global regulators such as IHF are starting to emerge. For example, the quorum-sensing regulator SmcR of *Vibrio vulnificus* binds to a distant sequence motif located around position −196 upstream from the *vvpE* gene coding for elastase and requires IHF to get closer to the promoter (33). The response regulator NarL, together with FNR, was shown to counteract IHF and Fis repression, but not H-NS, on the *E. coli nir* promoter (8); however, IHF can also act as a positive regulator of the *nir* promoter depending on the position of its binding sites (9). *Vibrio harveyi* LuxR binds to a distant site on the *lux* operon, although it has not been reported whether IHF aids in the activation of this promoter (68). Future studies are required to establish if additional regulatory proteins participate in the control of the *ecp* operon or if EcpR binds to an effector molecule to undergo structural changes that render a more effective EcpR protein *in vivo*. In this regard, it was recently reported

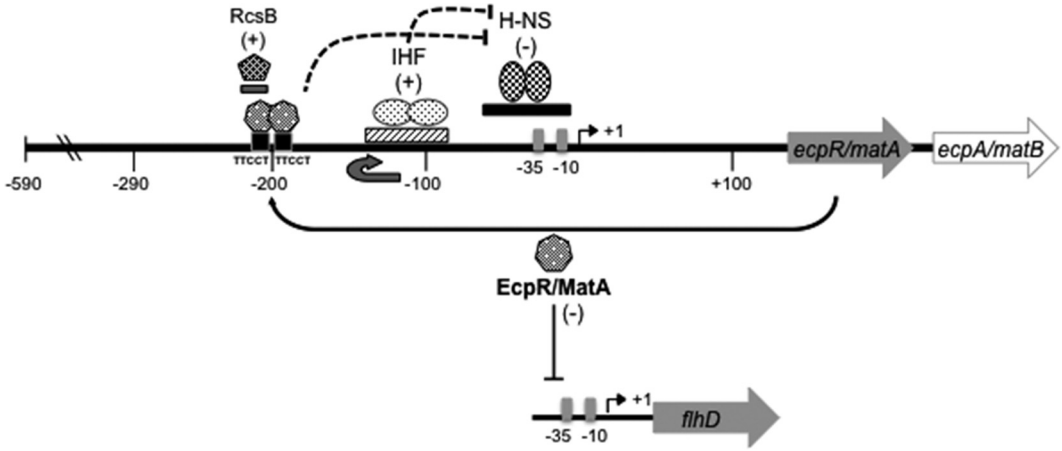

FIG 8 Transcriptional regulation of the *ecp* (*mat*) operon. *ecp* (*mat*) codes for EcpR/MatA, a regulatory protein containing a LuxR_C-like DNA-binding HTH domain that regulates positively the expression of the *ecp* operon by binding to two TTCCT boxes distantly located at positions −211 to −207 (distal box) and −189 to −185 (proximal box) with respect to the TSS. EcpR and IHF, which most likely bends the DNA between the TTCCT boxes and the promoter to get EcpR into close proximity to the promoter, counteract the repression exerted by H-NS on the *ecp* (*mat*) promoter. In addition, the response regulator RcsB also positively regulates the *ecp* (*mat*) promoter by binding to a sequence that overlaps the distant TTCCT box (40). EcpR/MatA also acts as a negative regulator by repressing the expression of the flagellar master operon *flhDC* (39).

that the *ecp* (*mat*) promoter in meningitis-causing *E. coli* is regulated by the response regulator RcsB by interacting with a sequence motif that overlaps the distal TTCCT box (40) (Fig. 8). Further work is needed to determine the potential interplay between EcpR and RcsB during *ecp* transcriptional activation and also to define whether RcsB is equally essential for *ecp* activation in A/E pathogens since mutations in the putative RcsB-binding sequence that did not modify the TTCCT distal box or a deletion of the first half of this site did not affect EcpR-mediated activation of the *ecp* promoter. This will be particularly important considering that the *ecp* operon may be differentially regulated between *E. coli* pathotypes, as illustrated by the fact that while ECP is expressed in A/E *E. coli* even at 37°C (57, 61), in the MNEC strain expression is observed only at 20°C (40, 53) and no expression was detected for *E. coli* MG1655 (38).

The *ecp* operon has distinctive features that make it a very interesting model of study. In addition to having genes encoding a second pilin-like protein and a second chaperone (26, 38, 53, 57), it is regulated by an atypical LuxR/NarL/FixJ-like protein, EcpR, which recognizes two distant 5-bp direct repeats that do not resemble the dyad symmetry of most binding sites recognized by other members of the family. In addition, activation of the *ecp* promoter requires IHF, which together with EcpR efficiently overcome the repression exerted by H-NS (Fig. 8). In summary, here we describe the elements that are involved in the transcriptional regulation of *ecp* and the role of a novel member of the protein family containing the LuxR_C-like DNA-binding HTH domain.

ACKNOWLEDGMENTS

This work was supported by grants from Consejo Nacional de Ciencia y Tecnología (CONACyT) (60796 and 154287) and Dirección General de Asuntos del Personal Académico (IN227410) to J.L.P. and by grant number AI66012 from NIAID, NIH, to J.A.G. V.I.M.-S. and A.M.-L. were supported by scholarships from CONACyT (166620 and 173678, respectively).

We thank A. L. Erdem and M. A. Rendón for the RT-PCR analysis and their input at the early stages of this work and A. Vázquez, F. J. Santana and M. Fernández-Mora for excellent technical assistance. We are grateful to K. Juárez for experimental advice.

REFERENCES

1. **Agron PG, Ditta GS, Helinski DR.** 1993. Oxygen regulation of *nifA* transcription *in vitro*. Proc. Natl. Acad. Sci. U. S. A. **90**:3506–3510.
2. **Aravind L, Anantharaman V, Balaji S, Babu MM, Iyer LM.** 2005. The many faces of the helix-turn-helix domain: transcription regulation and beyond. FEMS Microbiol. Rev. **29**:231–262.
3. **Avelino F, et al.** 2010. The majority of enteroaggregative *Escherichia coli* strains produce the *E. coli* common pilus when adhering to cultured epithelial cells. Int. J. Med. Microbiol. **300**:440–448.
4. **Baga M, Goransson M, Normark S, Uhlin BE.** 1985. Transcriptional activation of a *pap* pilus virulence operon from uropathogenic *Escherichia coli*. EMBO J. **4**:3887–3893.
5. **Barba J, et al.** 2005. A positive regulatory loop controls expression of the locus of enterocyte effacement-encoded regulators Ler and GrlA. J. Bacteriol. **187**:7918–7930.
6. **Blackburn D, et al.** 2009. Distribution of the *Escherichia coli* common pilus among diverse strains of human enterotoxigenic *E. coli*. J. Clin. Microbiol. **47**:1781–1784.
7. **Blomfield IC, Calie PJ, Eberhardt KJ, McClain MS, Eisenstein BI.** 1993. Lrp stimulates phase variation of type 1 fimbriation in *Escherichia coli* K-12. J. Bacteriol. **175**:27–36.
8. **Browning DF, Cole JA, Busby SJ.** 2000. Suppression of FNR-dependent transcription activation at the *Escherichia coli nir* promoter by Fis, IHF and H-NS: modulation of transcription initiation by a complex nucleoprotein assembly. Mol. Microbiol. **37**:1258–1269.
9. **Browning DF, Cole JA, Busby SJ.** 2008. Regulation by nucleoid-associated proteins at the *Escherichia coli nir* operon promoter. J. Bacteriol. **190**:7258–7267.
10. **Bustamante VH, et al.** 2011. PerC and GrlA independently regulate Ler expression in enteropathogenic *Escherichia coli*. Mol. Microbiol. **82**:398–415.
11. **Campellone KG.** 2010. Cytoskeleton-modulating effectors of enteropathogenic and enterohaemorrhagic *Escherichia coli*: Tir, EspFU and actin pedestal assembly. FEBS J. **277**:2390–2402.
12. **Casadaban MJ.** 1976. Transposition and fusion of the *lac* genes to selected promoters in *Escherichia coli* using bacteriophage lambda and Mu. J. Mol. Biol. **104**:541–555.
13. **Choi SH, Greenberg EP.** 1991. The C-terminal region of the *Vibrio fischeri* LuxR protein contains an inducer-independent *lux* gene activating domain. Proc. Natl. Acad. Sci. U. S. A. **88**:11115–11119.
14. **Clegg S, Wilson J, Johnson J.** 2011. More than one way to control hair

growth: regulatory mechanisms in enterobacteria that affect fimbriae assembled by the chaperone/usher pathway. J. Bacteriol. **193**:2081–2088.
15. **Crater DL, Moran CP Jr.** 2001. Identification of a DNA binding region in GerE from *Bacillus subtilis.* J. Bacteriol. **183**:4183–4189.
16. **Darwin AJ, Tyson KL, Busby SJ, Stewart V.** 1997. Differential regulation by the homologous response regulators NarL and NarP of *Escherichia coli* K-12 depends on DNA binding site arrangement. Mol. Microbiol. **25**:583–595.
17. **Datsenko KA, Wanner BL.** 2000. One-step inactivation of chromosomal genes in *Escherichia coli* K-12 using PCR products. Proc. Natl. Acad. Sci. U. S. A. **97**:6640–6645.
18. **Donnenberg MS, et al.** 1993. Role of the *eaeA* gene in experimental enteropathogenic *Escherichia coli* infection. J. Clin. Invest. **92**:1412–1417.
19. **Doughty S, et al.** 2002. Identification of a novel fimbrial gene cluster related to long polar fimbriae in locus of enterocyte effacement-negative strains of enterohemorrhagic *Escherichia coli.* Infect. Immun. **70**:6761–6769.
20. **Ducros VM, et al.** 2001. Crystal structure of GerE, the ultimate transcriptional regulator of spore formation in *Bacillus subtilis.* J. Mol. Biol. **306**:759–771.
21. **Egan SM, Stewart V.** 1991. Mutational analysis of nitrate regulatory gene *narL* in *Escherichia coli* K-12. J. Bacteriol. **173**:4424–4432.
22. **Eisenstein BI, Sweet DS, Vaughn V, Friedman DI.** 1987. Integration host factor is required for the DNA inversion that controls phase variation in *Escherichia coli.* Proc. Natl. Acad. Sci. U. S. A. **84**:6506–6510.
23. **Finlay BB, Falkow S.** 1997. Common themes in microbial pathogenicity revisited. Microbiol. Mol. Biol. Rev. **61**:136–169.
24. **Gally DL, Rucker TJ, Blomfield IC.** 1994. The leucine-responsive regulatory protein binds to the *fim* switch to control phase variation of type 1 fimbrial expression in *Escherichia coli* K-12. J. Bacteriol. **176**:5665–5672.
25. **Gao R, Mack TR, Stock AM.** 2007. Bacterial response regulators: versatile regulatory strategies from common domains. Trends Biochem. Sci. **32**:225–234.
26. **Garnett JA, et al.** 2012. Structural insights into the biogenesis and biofilm formation by the *Escherichia coli* common pilus. Proc. Natl. Acad. Sci. U. S. A. **109**:3950–3955.
27. **Giron JA, Ho AS, Schoolnik GK.** 1991. An inducible bundle-forming pilus of enteropathogenic *Escherichia coli.* Science **254**:710–713.
28. **Hanzelka BL, Greenberg EP.** 1995. Evidence that the N-terminal region of the *Vibrio fischeri* LuxR protein constitutes an autoinducer-binding domain. J. Bacteriol. **177**:815–817.
29. **Hernandes RT, et al.** 2011. Fimbrial adhesins produced by atypical enteropathogenic *Escherichia coli* strains. Appl. Environ. Microbiol. **77**:8391–8399.
30. **Holden NJ, Gally DL.** 2004. Switches, cross-talk and memory in *Escherichia coli* adherence. J. Med. Microbiol. **53**:585–593.
31. **Humphries AD, et al.** 2003. The use of flow cytometry to detect expression of subunits encoded by 11 *Salmonella enterica* serotype Typhimurium fimbrial operons. Mol. Microbiol. **48**:1357–1376.
32. **Humphries RM, Armstrong GD.** 2010. Sticky situation: localized adherence of enteropathogenic *Escherichia coli* to the small intestine epithelium. Future Microbiol. **5**:1645–1661.
33. **Jeong HS, Kim SM, Lim MS, Kim KS, Choi SH.** 2010. Direct interaction between quorum-sensing regulator SmcR and RNA polymerase is mediated by integration host factor to activate *vvpE* encoding elastase in *Vibrio vulnificus.* J. Biol. Chem. **285**:9357–9366.
34. **Karmali MA, Steele BT, Petric M, Lim C.** 1983. Sporadic cases of haemolytic-uraemic syndrome associated with faecal cytotoxin and cytotoxin-producing *Escherichia coli* in stools. Lancet **i**:619–620.
35. **Kim SH, Kim YH.** 2004. *Escherichia coli* O157:H7 adherence to HEp-2 cells is implicated with curli expression and outer membrane integrity. J. Vet. Sci. **5**:119–124.
36. **Klemm P.** 1986. Two regulatory *fim* genes, *fimB* and *fimE*, control the phase variation of type 1 fimbriae in *Escherichia coli.* EMBO J. **5**:1389–1393.
37. **Lasaro MA, et al.** 2009. F1C fimbriae play an important role in biofilm formation and intestinal colonization by the *Escherichia coli* commensal strain Nissle 1917. Appl. Environ. Microbiol. **75**:246–251.
38. **Lehti TA, et al.** 2010. Mat fimbriae promote biofilm formation by meningitis-associated *Escherichia coli.* Microbiology **156**:2408–2417.
39. **Lehti TA, Bauchart P, Dobrindt U, Korhonen TK, Westerlund-Wikstrom B.** 2012. The fimbriae activator MatA switches off motility in *Escherichia coli* by repression of the flagellar master operon *flhDC.* Microbiology **158**:1444–1455.
40. **Lehti TA, Heikkinen J, Korhonen TK, Westerlund-Wikstrom B.** 2012. The response regulator RcsB activates expression of Mat fimbriae in meningitic *Escherichia coli.* J. Bacteriol **194**:3475–3485.
41. **Levine MM, et al.** 1978. Escherichia coli strains that cause diarrhoea but do not produce heat-labile or heat-stable enterotoxins and are non-invasive. Lancet **i**:1119–1122.
42. **Lin AV, Stewart V.** 2010. Functional roles for the GerE-family carboxyl-terminal domains of nitrate response regulators NarL and NarP of *Escherichia coli* K-12. Microbiology **156**:2933–2943.
43. **Low AS, et al.** 2006. Cloning, expression, and characterization of fimbrial operon F9 from enterohemorrhagic *Escherichia coli* O157:H7. Infect. Immun. **74**:2233–2244.
44. **Martinez-Laguna Y, Calva E, Puente JL.** 1999. Autoactivation and environmental regulation of *bfpT* expression, the gene coding for the transcriptional activator of *bfpA* in enteropathogenic *Escherichia coli.* Mol. Microbiol. **33**:153–166.
45. **Mayer MP.** 1995. A new set of useful cloning and expression vectors derived from pBlueScript. Gene **163**:41–46.
46. **Minogue TD, Wehland-von Trebra M, Bernhard F, von Bodman SB.** 2002. The autoregulatory role of EsaR, a quorum-sensing regulator in *Pantoea stewartii* ssp. *stewartii*: evidence for a repressor function. Mol. Microbiol. **44**:1625–1635.
47. **Mol O, Oudega B.** 1996. Molecular and structural aspects of fimbriae biosynthesis and assembly in *Escherichia coli.* FEMS Microbiol. Rev. **19**:25–52.
48. **Morett E, Fischer HM, Hennecke H.** 1991. Influence of oxygen on DNA binding, positive control, and stability of the *Bradyrhizobium japonicum* NifA regulatory protein. J. Bacteriol. **173**:3478–3487.
49. **Nasser W, Bouillant ML, Salmond G, Reverchon S.** 1998. Characterization of the *Erwinia chrysanthemi expI-expR* locus directing the synthesis of two N-acyl-homoserine lactone signal molecules. Mol. Microbiol. **29**:1391–1405.
50. **Nasser W, Reverchon S.** 2007. New insights into the regulatory mechanisms of the LuxR family of quorum sensing regulators. Anal. Bioanal Chem. **387**:381–390.
51. **Nataro JP, Kaper JB.** 1998. Diarrheagenic *Escherichia coli.* Clin. Microbiol. Rev. **11**:142–201.
52. **Nicholls L, Grant TH, Robins-Browne RM.** 2000. Identification of a novel genetic locus that is required for in vitro adhesion of a clinical isolate of enterohaemorrhagic *Escherichia coli* to epithelial cells. Mol. Microbiol. **35**:275–288.
53. **Pouttu R, et al.** 2001. *matB*, a common fimbrillin gene of *Escherichia coli*, expressed in a genetically conserved, virulent clonal group. J. Bacteriol. **183**:4727–4736.
54. **Proft T, Baker EN.** 2009. Pili in Gram-negative and Gram-positive bacteria - structure, assembly and their role in disease. Cell. Mol. Life Sci. **66**:613–635.
55. **Puente JL, Bieber D, Ramer SW, Murray W, Schoolnik GK.** 1996. The bundle-forming pili of enteropathogenic *Escherichia coli:* transcriptional regulation by environmental signals. Mol. Microbiol. **20**:87–100.
56. **Raibaud O, Richet E.** 1987. Maltotriose is the inducer of the maltose regulon of *Escherichia coli.* J. Bacteriol. **169**:3059–3061.
57. **Rendon MA, et al.** 2007. Commensal and pathogenic *Escherichia coli* use a common pilus adherence factor for epithelial cell colonization. Proc. Natl. Acad. Sci. U. S. A. **104**:10637–10642.
58. **Reyrat JM, David M, Blonski C, Boistard P, Batut J.** 1993. Oxygen-regulated in vitro transcription of *Rhizobium meliloti nifA* and *fixK* genes. J. Bacteriol. **175**:6867–6872.
59. **Richet E, Raibaud O.** 1989. MalT, the regulatory protein of the *Escherichia coli* maltose system, is an ATP-dependent transcriptional activator. EMBO J. **8**:981–987.
60. **Riley LW, et al.** 1983. Hemorrhagic colitis associated with a rare *Escherichia coli* serotype. N. Engl. J. Med. **308**:681–685.
61. **Saldana Z, et al.** 2009. The *Escherichia coli* common pilus and the bundle-forming pilus act in concert during the formation of localized adherence by enteropathogenic *E. coli.* J. Bacteriol. **191**:3451–3461.
62. **Saldana Z, et al.** 2009. Synergistic role of curli and cellulose in cell adherence and biofilm formation of attaching and effacing *Escherichia coli* and identification of Fis as a negative regulator of curli. Environ. Microbiol. **11**:992–1006.
63. **Saldana Z, Sanchez E, Xicohtencatl-Cortes J, Puente JL, Giron JA.** 2011.

Surface structures involved in plant stomata and leaf colonization by shiga-toxigenic *Escherichia coli* O157:H7. Front. Microbiol. **2**:119.
64. **Samadder P, et al.** 2009. The *Escherichia coli ycbQRST* operon encodes fimbriae with laminin-binding and epithelial cell adherence properties in Shiga-toxigenic *E. coli* O157:H7. Environ. Microbiol. **11**:1815–1826.
65. **Sanger F, Nicklen S, Coulson AR.** 1977. DNA sequencing with chain-terminating inhibitors. Proc. Natl. Acad. Sci. U. S. A. **74**:5463–5467.
66. **Soto GE, Hultgren SJ.** 1999. Bacterial adhesins: common themes and variations in architecture and assembly. J. Bacteriol. **181**:1059–1071.
67. **Stevens AM, Dolan KM, Greenberg EP.** 1994. Synergistic binding of the *Vibrio fischeri* LuxR transcriptional activator domain and RNA polymerase to the *lux* promoter region. Proc. Natl. Acad. Sci. U. S. A. **91**:12619–12623.
68. **Swartzman E, Meighen EA.** 1993. Purification and characterization of a poly(dA-dT) *lux*-specific DNA-binding protein from *Vibrio harveyi* and identification as LuxR. J. Biol. Chem. **268**:16706–16716.
69. **Tarr PI, et al.** 2000. Iha: a novel *Escherichia coli* O157:H7 adherence-conferring molecule encoded on a recently acquired chromosomal island of conserved structure. Infect. Immun. **68**:1400–1407.
70. **Torres AG, et al.** 2002. Identification and characterization of *lpfABCC′DE*, a fimbrial operon of enterohemorrhagic *Escherichia coli* O157:H7. Infect. Immun. **70**:5416–5427.
71. **Torres AG, et al.** 2006. Outer membrane protein A of *Escherichia coli* O157:H7 stimulates dendritic cell activation. Infect. Immun. **74**:2676–2685.
72. **Tsai CS, Winans SC.** 2010. LuxR-type quorum-sensing regulators that are detached from common scents. Mol. Microbiol. **77**:1072–1082.
73. **van der Woude MW, Braaten BA, Low DA.** 1992. Evidence for global regulatory control of pilus expression in *Escherichia coli* by Lrp and DNA methylation: model building based on analysis of *pap*. Mol. Microbiol. **6**:2429–2435.
74. **Van Houdt R, Michiels CW.** 2005. Role of bacterial cell surface structures in *Escherichia coli* biofilm formation. Res. Microbiol. **156**:626–633.
75. **White CE, Winans SC.** 2007. The quorum-sensing transcription factor TraR decodes its DNA binding site by direct contacts with DNA bases and by detection of DNA flexibility. Mol. Microbiol. **64**:245–256.
76. **White-Ziegler CA, Angus Hill ML, Braaten BA, van der Woude MW, Low DA.** 1998. Thermoregulation of *Escherichia coli* pap transcription: H-NS is a temperature-dependent DNA methylation blocking factor. Mol. Microbiol. **28**:1121–1137.
77. **Xicohtencatl-Cortes J, et al.** 2007. Intestinal adherence associated with type IV pili of enterohemorrhagic *Escherichia coli* O157:H7. J. Clin. Invest. **117**:3519–3529.